Analytical Chemistry in Molecular Electronics

Adam Johan Bergren[1] and Richard L. McCreery[2]

[1]National Institute for Nanotechnology, National Research Council Canada, Edmonton, Alberta T6G 2M9, Canada; email: adam.bergren@nrc.ca

[2]Department of Chemistry, University of Alberta, Edmonton, Alberta T6G 2M9, Canada; email: richard.mccreery@ualberta.ca

Annu. Rev. Anal. Chem. 2011. 4:173–95

First published online as a Review in Advance on March 3, 2011

The *Annual Review of Analytical Chemistry* is online at anchem.annualreviews.org

This article's doi: 10.1146/annurev-anchem-061010-113847

1936-1327/11/0719-0173$20.00

Keywords

molecular junction, buried interfaces, electronics, electrochemistry, microscopy, spectroscopy

Abstract

This review discusses the analytical characterization of molecular electronic devices and structures relevant thereto. In particular, we outline the methods for probing molecular junctions, which contain an ensemble of molecules between two contacts. We discuss the analytical methods that aid in the fabrication and characterization of molecular junctions, beginning with the confirmation of the placement of a molecular layer on a conductive or semiconductive substrate. We emphasize methods that provide information about the molecular layer in the junction and outline techniques to ensure molecular layer integrity after the complete fabrication of a device. In addition, we discuss the analytical information derived during the actual device operation.

1. INTRODUCTION

The term molecular electronics (ME) refers to a broad range of devices, structures, and experimental paradigms that share some common themes. The possibility of incorporating molecules into electronic circuits has major scientific and commercial potential, given that a wide range of electronic properties, energy levels, conductivity, and so on are available from the vast array of chemical structures that could be integrated into microelectronic devices (1–11). In addition to the advantage of their inherently small size, molecules may enable a variety of electronic functions that are not readily attainable with inorganic semiconductors, such as chemical sensing, low power consumption, flexibility, and lower cost. If this promise is to be realized, however, new analytical probes are necessary to characterize molecular electronic devices, and in many cases the analytical requirements are demanding (12). For example, a common device in ME is the molecular junction, which consists of an approximately <1–5-nm-thick molecular layer oriented between two conducting contacts (**Figure 1**), with a device area ranging from ~1 mm^2 to well below 1 μm^2 (1, 4, 7, 8, 13). To fully characterize a molecular junction, the analytical probe must provide information about the molecular structure and dynamics of a sample with a thickness of a few nanometers and an area of <1 to >10,000 μm^2, inside possibly opaque metallic contacts, often during application of a voltage bias and current measurement on a nanosecond-dc timescale. In an illustration of the importance of the problem, a 2007 National Science Foundation workshop entitled Building Electronic Function into Nanoscale Molecular Architectures identified as a primary research goal to "develop time-resolved optical spectroscopies and imaging schemes to probe molecular structure in operating devices" (14, p. 19).

Space constraints dictate some choices about which analytical aspects of ME to consider in this review: We emphasize the analytical characterization of the chemical structure of the ultrathin molecular layers used in ME. Although the electronic properties of devices are often considered in conjunction with these characterizations in order to derive meaningful insights into structure–electronic function relationships, we do not focus on the electronic properties. ME is often separated into single-molecule and ensemble paradigms; the latter deals with molecular layers of 10^3 to 10^{12} molecules that are often oriented in parallel (13). Elegant theory and experiments on the electronic properties of single molecules (15–21), including those described in a recent Annual Reviews article (22), have been reported and reviewed. The vast majority of single-molecule experiments involve scanning-probe microscopy and are not discussed here, except for the case of inelastic tunneling spectroscopy (IETS) in Section 3. Organic electronics is a rich research area involving molecular layers much thicker than molecular dimensions—generally 100–1,000 nm. Various analytical techniques have been applied to organic electronic devices, including electronic (23) and vibrational spectroscopy (24), but the behavior and electron transport in such thick layers are probably fundamentally different from those in single molecules or thin molecular layers. The focus of this review is on ensemble molecular junctions, whose areas are large enough to permit optical spectroscopy. In Section 2, we describe analytical methods for characterizing molecular junctions during fabrication, including substrates, molecular layers, and top contacts, and in Section 3, we discuss analytical probes of finished molecular devices, including live monitoring of the structure and dynamics during operation with an applied bias.

2. FABRICATION AND CHARACTERIZATION

Fabrication of a molecular junction involves making electrical contact to both sides of a molecular layer; this process can be thought of as wiring a molecule (**Figure 1*a***). However, the solder used to wire a molecular layer that is less than 10 nm thick certainly cannot be applied using a

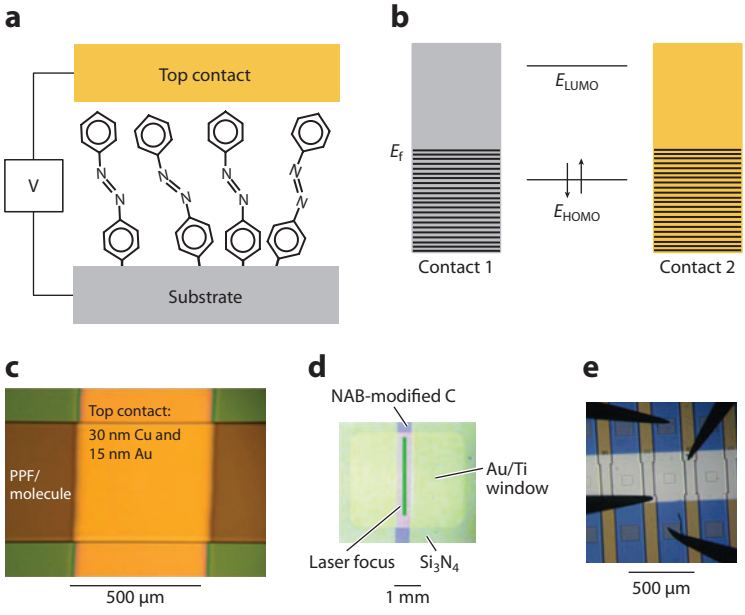

Figure 1

(*a*,*b*) Examples of molecular electronics (ME) devices. (*a*) A two-terminal ME junction consisting of a molecular layer of azobenzene molecules bonded to a conductive C substrate with a metallic top contact. (*b*) Energy-level diagram of a two-terminal junction, where the molecular HOMO and LUMO are possible conduction pathways and E_f is the Fermi level of the contact(s). (*c*–*e*) Optical micrograph images of actual ME devices. (*c*) A C/NAB/Cu/Au cross junction. Reproduced with permission from Reference 40. Copyright IOP, Ltd. (*d*) An ME junction with partially transparent top contacts suitable for Raman spectroscopy. Reproduced with permission from Reference 87. Copyright American Chemical Society. (*e*) A microfabricated C/molecule/Cu molecular junction (140). Abbreviations: NAB, nitroazobenzene; PPF, pyrolyzed photoresist film, a form of conductive carbon (C).

macroscopic iron: Technically advanced nanofabrication methods are required to successfully produce a molecular junction (2, 8, 9, 25–27). Because direct visual inspection of the conductor to molecule contacts in nanoscopic junctions cannot be readily carried out, careful analysis is required to confirm junction structure. In addition, there are several aspects of molecular junctions that require more information than that provided by a simple visual inspection: One must obtain information about the molecular orientation, modes of interfacial binding and/or interaction between the contacts and the molecules, molecular layer thickness, and any possible structural defects in the junction. These factors affect the energetics of the contacts with respect to the molecular orbitals (**Figure 1*b***), which, in turn, determine the nature of electron transport through the junction. For these characterizations to be performed, the molecular layers may be characterized on the substrate before the junction is completed, or when possible, the analysis can be carried out using a junction structure that is amenable to optical characterization (**Figures 1*d*, 2**).

A description of the full details of the many methods used to construct molecular junctions is beyond the scope of this review; we refer the reader to other publications (e.g., 2, 8, 9, 13, 25–36). However, several features are common to most types of junctions. For example, some method of incorporating the molecule into the junction is needed, and the circuit must be completed by use of two contacts. The type of material used for the bottom contact often determines the mode of binding for the molecular layer, which can also determine the degree of electronic coupling

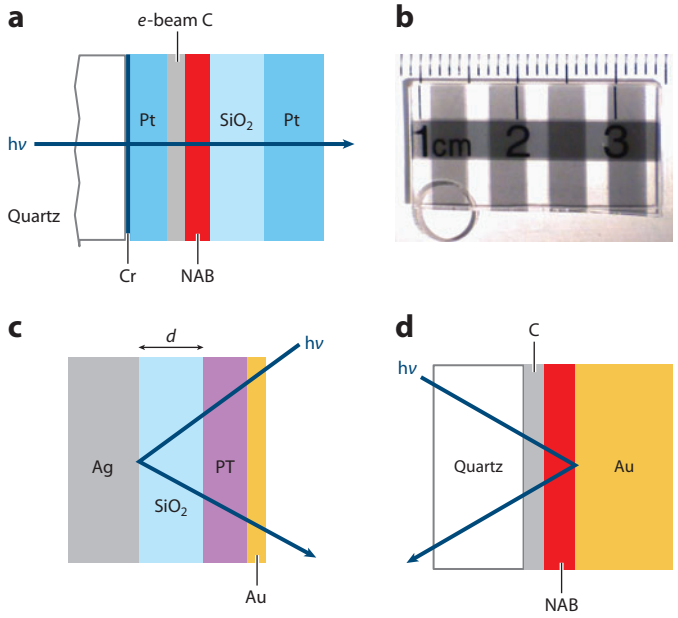

Figure 2

Molecular junctions configured for spectroscopic characterizations by use of different techniques and geometries. (*a*) Transmission device with layer thicknesses as follows. (*From left to right*) Quartz substrate (~1 mm), Cr (1 nm), Pt (5 nm), *e*-beam C (5 nm), nitroazobenzene (NAB) (4.5 nm), SiO_2 (10 nm), and Pt (10 nm). (*b*) Photograph of four optically transparent molecular junctions of the structure shown in panel *a* on a ruler, illustrating partial transparency. Reproduced with permission from Reference 91. Copyright American Chemical Society. (*c*,*d*) Molecular junction configurations suitable for reflection or scattering techniques are shown for two cases. (*c*) Configuration using partially transparent top contacts for investigation of a Ag/SiO_2/polythiophene (PT)/Au molecular junction, where *d* indicates the SiO_2 thickness. (*d*) Configuration using partially transparent substrate materials (84).

between the contact and the molecular layer and its stability. In addition, the properties of the substrate can strongly affect the electronic nature of the device. For example, a semiconducting bottom contact yields a fundamentally different electronic response than a metallic contact, even when all other variables are constant. As we discuss below, verification of chemical bonding, molecular layer ordering, and orientation can and must be assessed through the use of a variety of analytical methods, including optical spectroscopy.

The electronic properties of molecular junctions (see Section 3) may be investigated through various means (37); one of the most common and useful is the current–voltage (*i-V*) characteristic. Obviously, the *i-V* behavior of a molecular electronic device bears directly on its applications, but electronic behavior can also reveal aspects of junction structure and transport mechanism. However, any theories that attempt to describe the *i-V* behavior for a given mechanism must rely on so-called geometric boundary conditions that are intimately related to the detailed chemical and physical structure of the junction. In Section 2, we describe several analytical techniques for characterizing molecular electronic devices, both during fabrication to confirm structure and in completed devices to determine the fate of the molecular layer after fabrication steps. We illustrate several types of optical spectroscopy (**Figure 2**) and electron microscopy and provide examples for each step of the junction fabrication process. Finally, in Section 3, we discuss methods for examining different aspects of the molecule in a live junction (i.e., in situ methods).

2.1. Substrates

The first component of a junction is typically the substrate upon which the molecules will reside; it can be constructed through various techniques. The use of a flat conductor or semiconductor for the bottom contact is a common approach that often involves vapor deposition of metals on Si or SiO_2 (38–51). Alternatively, lithographically generated structures (52, 53) can be used to form nanogaps in conductors such that when molecules bridge the gap, charge flows through or across the molecular layer. In the first case, the bottom contact can consist of commercially available Si wafers (51), template-stripped metal surfaces (42), or a conducting C film (41). Taking a molecular cross-junction (**Figure 1**) as an example, the bottom contact for use in a molecular junction must meet several requirements that can be assessed with analytical techniques. The substrate must have suitable electrical conductivity and should be flat on the nanoscale (generally, topographical features must be smaller than the vertical dimensions of the molecular layer that is to be attached). For this type of substrate, the physical nature of the contact can be investigated before the application of a molecular layer through the use of imaging techniques (54), optical spectroscopy (55), or other methods. Roughness can be evaluated via scanning-probe microscopy (56); scanning tunneling microscopy and atomic force microscopy (AFM) provide height resolution in the ~0.1-nm range. Electrical conductivity can be assessed via standard electrical testing techniques for macroscopic contacts (e.g., the four-point probe).

2.2. Molecular Layers

Ideally, the active component of a molecular junction should be the molecule itself, but this is not always the case. Instead, a molecular junction should be considered a system that includes the molecule and the contacts. The electronic signature(s) of the molecular component can thus be deduced from careful study of the system. Variation of molecular structure and the way in which contact is made help to form complete views of the factors that control charge transport in ME. There are numerous ways to apply a molecular layer to a surface (57–59), and many have been used to construct molecular junctions. For the case of a flat conductor used as a bottom contact, Langmuir-Blodgett films (44), self-assembled monolayers (42, 43), and covalently bonded layers (40, 41, 60) have been studied in detail. Because the electronic behavior and electron transport of the molecular device depend strongly on the bonding and orientation of the molecular layer, it is important to learn as much as possible about the detailed structure of the molecular layer on the substrate. Factors such as the degree of electronic coupling, tunneling barrier formation, and contact resistance often depend on the specific molecule-to-substrate bond and the arrangement of substrate atoms at the bonding site (15, 17, 19, 61). Methods for analyzing these parameters can begin with a simple confirmation of the presence of the molecular layer, then proceed to the acquisition of more detailed information via a variety of imaging and spectroscopic techniques.

AFM has been used to assess both the roughness of the substrate and molecular layer and the thickness of the molecular layer by observing profiles through a deliberate scratch in the layer (56). In addition, the nucleation and growth of molecular layers on C substrates, notably the formation of multilayers when aggressive surface modification is used (62, 63), have been monitored through the use of AFM. IR spectroscopy has been used, in conjunction with AFM (63), to confirm the molecular structure. Through these characterizations, the nucleation and growth mechanism of molecular layers deposited via the electrochemical reduction of diazonium reagents has been described in detail. This knowledge has made it possible to control the thickness of the adlayer with subnanometer resolution, enabling fundamental studies of charge transport in ME devices (41).

In addition to morphology, height, and thickness information, related imaging techniques can be used to investigate the electrical properties of molecular layers on surfaces. Kelvin probe microscopy (64, 65), along with the closely related technique electric force microscopy (66, 67), uses a conductive probe to investigate the electronic properties of surfaces. This type of imaging mode measures the potential difference between the tip and the sample (i.e., the work function difference for a conductive sample and the surface potential for a nonconductive sample). The measurements are based on the formation of a capacitor with the surface under study (i.e., the probe forms one plate of the capacitor and the sample forms the second), and the voltage required to balance the charge on the opposite plates of the capacitor is measured, which yields the potential difference between the sample and the tip. These measurements can provide information about the change in work function as the molecular structure is varied (65), as well as correlations between surface dipole and energy-level alignment (68) and the spectroscopic properties (69) of the molecular layer. To obtain more detailed information about molecular structure, numerous spectroscopic tools have been applied.

Photoelectron spectroscopies have a high surface sensitivity that makes them attractive options for characterizing thin molecular layers. Furthermore, there are various modes of operation that can provide information about different aspects of a molecular device. X-ray photoelectron spectroscopy (XPS) is often used to verify that the intended functional groups remain intact after fabrication of the junction (70, 71). In addition, XPS can provide information about the oxidation state of the top-contact materials (40, 70, 72–74) and about interactions between the molecular layer and the top contacts (75–78). With a UV source [ultraviolet photoelectron spectroscopy (UPS)], valence-level rather than core-level orbitals can be probed, which yields insights into the alignment of contact energy levels and molecular orbitals, as well as the work function of the sample. UPS is often used to understand the energetics of valence-level molecular orbitals for molecular structures adsorbed onto a conductive substrate (40, 79–81). These measurements are especially useful because they enable assessments of the energy-level alignment of the contact Fermi level and the molecular orbitals, which is a parameter that dictates the efficiency of charge transport in many transport models. The offset between the contact Fermi level (E_f) and the molecular HOMO and LUMO energies (**Figure 1*b***) can correspond to a tunneling barrier, as described by the Simmons model (41), or can be used to describe the efficiency of transmission through conducting channels in the Landauer approach (82).

Vibrational spectroscopy [e.g., Fourier transform IR (FTIR), Raman] has been used to verify chemical structure in molecular junctions at various points during fabrication. **Figure 3** shows an example for functionalized alkanes at Si (70). This type of analysis is important in the fabrication of a molecular device, as it confirms that the surface has been modified with the intended molecule. For Si substrates, FTIR also provides an excellent marker for the formation of a surface oxide.

In combination with a transparent support, vibrational spectroscopy can be applied to so-called buried interfaces, where the molecule of interest is sandwiched between the two contact layers in completed devices (50, 83, 84). Such experiments are extremely valuable because they provide information about the molecule after the top contact has been deposited. Thus, these experiments can be used to investigate any structural changes induced from the deposition of top-contact materials onto the molecule. In the case of Si substrates, one can obtain Si wafers with high transparency in the IR region of the electromagnetic spectrum. Following application of a highly reflective top-contact metal with a suitable optical density, a reflection IR spectrum can be obtained by passing the beam through the partially transparent Si support. **Figure 4** shows an example of IR spectra obtained with this technique for 4-nitrobenzene (**Figure 4*a***) and 2-methoxy-4-nitrobenzene (**Figure 4*b***) molecules chemisorbed onto Si (50). In this study, two methods for top-contact deposition were used, with strikingly different results. First, direct evaporation of

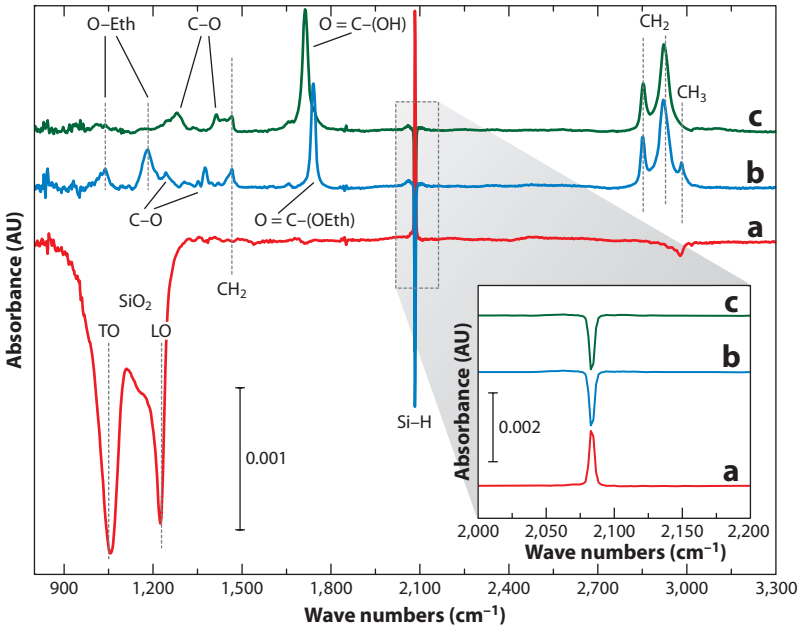

Figure 3

(*a*) Fourier transform IR absorption spectra of a hydrogenated Si(111) surface. A peak for the Si–H stretch is observed at 2,083 cm^{-1}, along with negative peaks at 1,055 cm^{-1} for the transverse optical (TO) and 1,224 cm^{-1} for the longitudinal optical (LO) modes of SiO_2. The negative intensities at 1,224 and 1,055 cm^{-1} arise because the spectra for the H-terminated surface is referenced to a sample with native oxide. (*b*) Spectrum of a COOEth-terminated self-assembled monolayer (SAM) on Si (referenced to the Si–H surface), following chemisorption of the ethyl ether–terminated alkane. Peaks for the appropriate functional groups indicate that the surface has been effectively modified. (*c*) Spectrum for a COOH-terminated SAM (referenced to the Si–H surface) generated by removal of the ethyl ether group, which is used as a protective group during the surface-modification step. (*Inset*) Zoomed-in view of the Si–H vibration modes on the different surfaces. Reproduced with permission from Reference 70. Copyright American Chemical Society.

100 nm of Au onto either molecule led to complete loss of the vibrational features associated with the molecules, as shown by the top spectra in **Figure 4*a*,*b***. Next, the indirect (or soft) evaporation of the same thickness of Au (carried out in Ar and in a geometry such that the Au atoms impinged the molecular surface only after undergoing collisions to reduce kinetic energy) resulted in clear features associated with the molecular layer, as shown by the middle spectra in **Figure 4*a*,*b***. There was a slight reduction in intensity, which was attributed to metallization-induced decomposition. In this case, the molecular layers were grafted to the Si via the electrochemical reduction of diazonium reagents, which resulted in a Si–C bond (85, 86). Clearly, the direct deposition of Au is not suitable for fabricating an electronic junction with the conditions employed in this experiment, which demonstrates that careful analytical characterization is critical in ME.

An alternative to FTIR for obtaining vibrational information is Raman spectroscopy. Although this technique has a relatively low sensitivity, it has been successfully employed in numerous experiments (52, 74, 87–89). For example, Raman spectroscopy was used to verify the integrity of a molecule after the direct deposition of 50 nm of Ag (84). **Figure 5** shows an overlay of the Raman spectra for a molecular layer of nitroazobenzene (NAB) on a partially transparent support (Ti on quartz) before and after deposition of a 50-nm layer of Ag. In this case, the molecular layer was deposited by the spontaneous reduction of a diazonium reagent by a thin (5-nm) primer layer

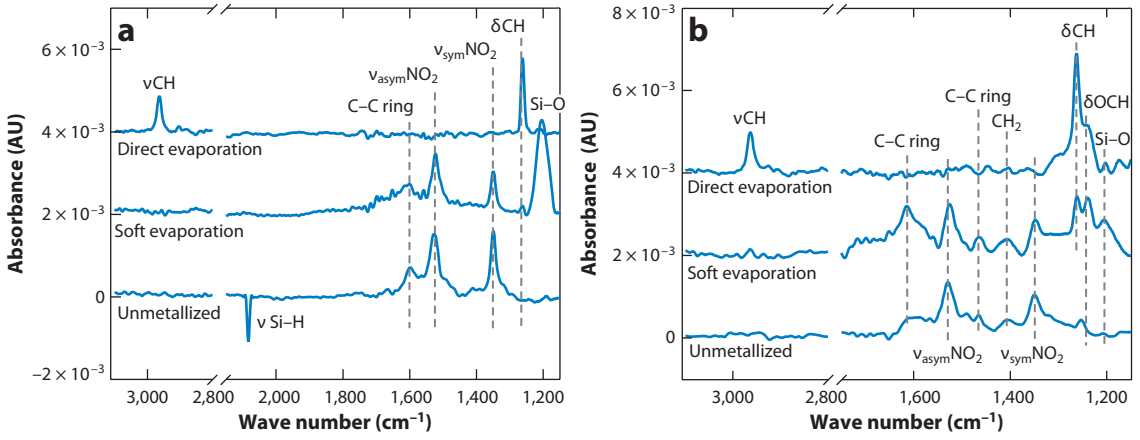

Figure 4

Fourier transform IR spectra of Si surfaces modified with (*a*) 4-nitrobenzene and (*b*) 2-methoxy-4-nitrobenzene before (*bottom*) and after metal deposition using Ar backfill soft evaporation (*middle*) and standard electron-beam evaporation (*top*). The unmetallized spectra were collected in transmission mode, whereas the metallized sample spectra were obtained by passing the IR beam through the partially transparent Si substrate. Reproduced with permission from Reference 50. Copyright American Chemical Society.

of Ti on quartz. The Raman spectra were obtained through the transparent quartz substrate. The spectra of the molecular layer before and after the deposition of Ag are similar; the change in relative peak intensity is attributable to the partial reduction of NAB (72, 87, 90). These results illustrate that with a different metal and substrate, a molecular layer can survive direct deposition of metals without major structural changes. The results presented in **Figures 4** and **5** therefore indicate that analytical characterization is needed to determine (*a*) whether the molecular component remains intact after metal deposition and (*b*) that many variables (e.g., details of the deposition conditions, type of metal, mode of binding, substrate identity) probably determine the result (13).

UV-visible spectroscopy provides valuable information about the electronic transitions in a molecular layer (91, 92), and as such is a direct probe of the energetics of molecular electronic

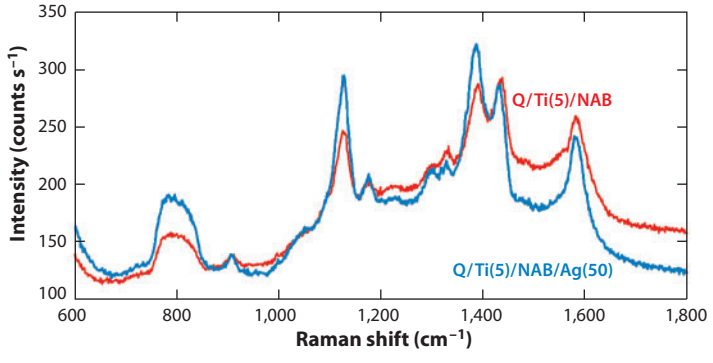

Figure 5

Raman spectra (514.5-nm excitation) obtained through a quartz (Q) substrate (as in **Figure 2*d***) for a nitroazobenzene (NAB) layer on a 5-nm layer of Ti on Q. The red curve was obtained before metal deposition; the blue curve was obtained after direct deposition of 50 nm of Ag by electron-beam evaporation. Reproduced with permission from Reference 84. Copyright American Chemical Society.

junctions. Conventional spectrometers can readily be used to obtain spectra from thin molecular layers adsorbed onto partially transparent substrates (55, 93). A particularly important result obtained from UV-visible spectroscopy of molecular junctions involves changes in the absorbance spectrum for a molecular layer when it was chemisorbed onto a substrate, relative to the free molecule in solution (55). In this case, a redshift was observed for a layer of NAB on optically transparent C relative to the free molecule, which indicated that some perturbation of the molecular orbitals took place. As we discuss below, these changes in UV-visible spectra, which arise from an applied voltage bias, can also be used to study redox reactions in a live junction.

Finally, mass spectrometry has also been applied to the study of molecular junctions (78). This experiment showed that thermally evaporated Au atoms penetrate self-assembled monolayers but that specific chemical effects can be used to control the interaction of Au atoms with appropriate end functionalities (78).

2.3. Top Contacts

There are several ways to apply top contacts to a molecular junction. Some types of molecular junctions either do not require a top contact (e.g., nanogap junctions) or are made using a scanning tunneling microscopy (9) or conducting-probe AFM tip (94–96). AFM has also been used to assess the progression of top-contact deposition (97, 98). Top-contact materials can be applied by vapor deposition of metals, as long as care is taken to ensure the integrity of the molecular layer (as described in the previous section). However, many other approaches have been used to make a top contact without subjecting the molecular layer to the often harsh conditions of vapor deposition. For example, conducting polymers have been used to make direct contact with the molecular layer, thereby providing a buffer between the impinging vapor-deposited metal atoms and the molecular layer (1). The conducting polymer maintains a high electrical conductivity such that the junctions can be treated as metal/molecule/metal devices. A recent variation on metal deposition is an indirect technique in which Au, Cu, or Pt atoms are deposited adjacent to the molecular layer, then diffuse onto the molecules to make electrical contact. When this surface diffusion–mediated deposition (SDMD) (99) technique was applied, the metal atoms dissipated most of their energy before touching the molecules. In addition, the investigators observed the *i-V* behavior during metal deposition to determine whether any changes took place during the course of junction formation. Importantly, the *i-V* curves obtained with SDMD were very similar to those obtained from junctions made with direct metal deposition for the case of diazonium-derived molecular layers on C surfaces and Cu top contacts.

Although optical microscopy is useful for illustrations such as **Figure 1*e***, the dimensions of most molecular junctions require electron microscopy to probe junction structure. **Figure 6** shows several examples of electron microscopy applied to C/molecule/metal junctions. **Figure 6*a*** is a scanning electron microscopy (SEM) image of a sample that was cleaved through the junction and subsequently positioned so that the exposed edge could be observed. The substrate layers and curvature of the C were readily observed, although the ~4-nm-thick NAB layer was too thin for SEM resolution. **Figure 6*b*** is an SEM image of a C/polypyrrole/TiO_2/Au sample that was cut with a focused ion beam to make a thin (10–100-nm) slice through the junction region. This section was then removed, mounted, and rotated for transmission electron microscopy (TEM); the thin dimension was oriented along the TEM beam axis to obtain a cross-sectional view (**Figure 6*c***). In this experiment, TEM confirmed the polypyrrole, TiO_2, and Au layer thicknesses, and electron energy-loss spectroscopy provided elemental composition. Additional examples of electron microscopy used for molecular junctions include the observation of conducting filaments

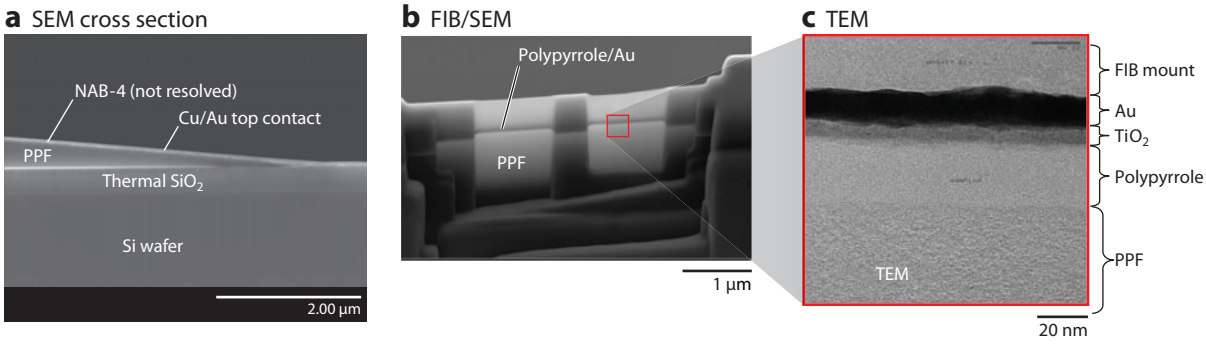

Figure 6

Micrographs of finished molecular junctions obtained with scanning electron microscopy (SEM) and transmission electron microscopy (TEM). (*a*) SEM image cross section of a PPF/NAB/Cu/Au junction cleaved through the junction region (40, 41, 140). (*b*) SEM image of a thin slice of a junction prepared by a focused ion beam (FIB) prior to mounting for TEM. (*c*) TEM image of a PPF/polypyrrole/TiO_2/Au molecular junction (141). Abbreviations: NAB, nitroazobenzene; PPF, pyrolyzed photoresist film, a form of conductive carbon.

(100), the penetration of an Au top contact into the molecular layer (101), and the imaging of a high-density molecular memory device (4).

With the notable exception of SDMD, the characterizations discussed so far involve the ex situ (and, in some cases, destructive) assessment of substrates, molecular layers, contacts, and complete junctions. However, the use of junctions that are amenable to optical probing in a completed, working device (**Figure 2**) can yield invaluable information about transport mechanisms, junction stability, and even chemical reactions that occur during the application of a voltage. In Section 3, we discuss several examples of in situ optical spectroscopy of active molecular junctions.

3. MONITORING WORKING MOLECULAR JUNCTIONS

Electronic characterization methods such as monitoring of *i-V* behavior and impedance analysis are similar to those used in electrochemistry and semiconductor-device characterization. These approaches do not provide direct information about molecular structure, but they are critical to analyzing device behavior. When these approaches are combined with spectroscopic methods, correlations between structural features and electronic performance can be assessed. In any electronic measurement of a molecular junction, precautions should be taken to ensure that the programmed voltage is applied across the molecular layer. Although this process may appear trivial, the conductors used for both bottom and top contacts are often very thin (~15 nm), and the probes used to make contact with the conductors cannot always be placed close to the junction. These factors can render the resistance of the leads and contact probes significant enough to cause ohmic potential errors (i.e., an *iR* drop) that interfere with the electrical measurement. Thus, when the resistance of the junction is smaller than or even comparable to the resistance of the leads, a simple two-wire measurement for applying a voltage bias and measuring the resulting current (**Figure 7*a***) results in less than the programmed voltage being applied to the junction. For such cases, instrumentation has been developed to correct the lead resistance in one contact (**Figure 7*b*,*c***) and both leads (**Figure 7*d***). To illustrate how these measurement modes act to correct for ohmic potential errors, we consider the case for both active and passive correction. The passive three-wire mode (**Figure 7*b***) uses a high-impedance voltage monitor to determine the actual applied voltage at a second lead placed outside the current path. The voltage axis is corrected for ohmic losses, but

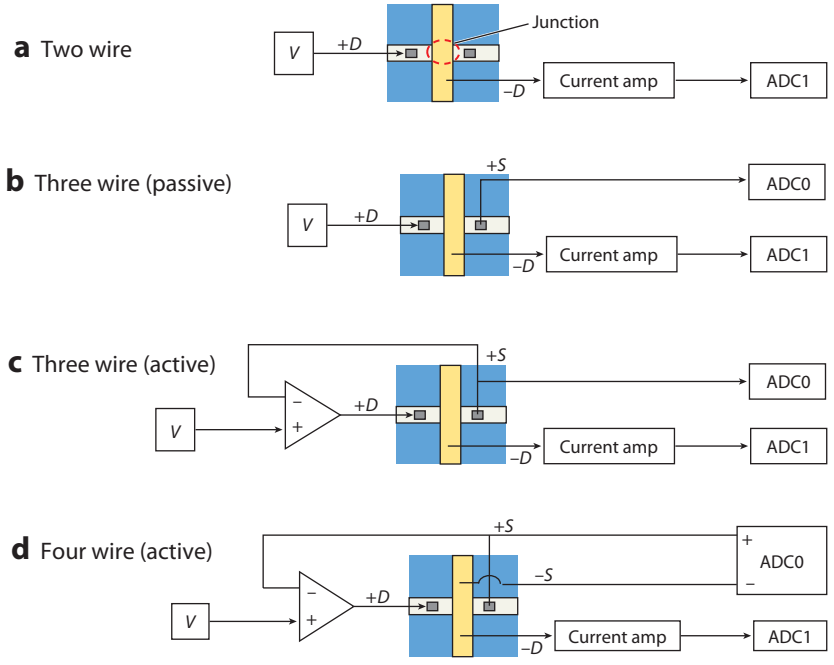

Figure 7

Wiring schematics for (*a*) two-, (*b*,*c*) three-, and (*d*) four-wire measurements of current–voltage (*i-V*) behavior of molecular junctions. *V* refers to the bias voltage from a digital-to-analog converter, and ADC1 stands for the analog-to-digital channel for current. ADC0 monitors voltage and has a differential input in the case of the four-wire arrangement. *D* and *S* denote drive and sense, respectively; the *S* leads correspond to high-impedance voltage monitors.

the applied voltage does not reach the programmed value (i.e., if *iR* is 0.2 V, then a programmed voltage of 1 V yields a reading of 0.8 V at the input of the voltmeter). The active three-wire mode (**Figure 7*c***) uses an operational amplifier to compensate for ohmic losses by increasing the drive voltage—a technique commonly employed in electrochemistry in three-electrode potentiostats. This mode controls the applied voltage to the desired value but does not correct for ohmic losses in the lead to the current amplifier. However, an active four-wire mode (**Figure 7*d***) with two sense leads and a differential monitor of the applied voltage corrects for both ohmic losses in both the top and bottom leads of the molecular junction and losses at the connections to the instrument. Obtaining an accurate correction for such losses depends on the use of high-impedance voltage monitors and assumes that there is a negligible potential gradient across the lateral dimension of the junction itself. There are numerous instruments that can operate in two-, three-, and four-wire modes. Commercially available potentiostats for use in electrochemical measurements can be used; although they are not typically capable of the four-wire mode, most can operate in the three-wire mode (102). Other commercial instrumentation used in the semiconductor industry, such as source measurement units and high-impedance electrometers, is often supplied with two- and four-wire modes. Custom-built instrumentation is also often used; such instruments have the advantage of flexibility in configuration (72, 103).

As mentioned above, determination of the structure and dynamics of completed molecular electronic devices is often challenging due to the need to probe very thin molecular layers that are often buried beneath opaque conductors (12). Because it is the presence of the organic molecule

that distinguishes ME from conventional microelectronics, below we emphasize nondestructive characterization techniques that provide information about molecular structure, in some cases dynamically. To date, these techniques include UV-visible absorption spectroscopy, FTIR and Raman spectroscopy, and IETS. The optical techniques require some level of transparency of either (*a*) the top or bottom contact in the case of reflection or scattering geometry or (*b*) the entire junction in the case of a transmission experiment (**Figure 2**). Fortunately, the techniques developed for spectroelectrochemistry (104, 105), which involve transparent conductors, are directly applicable to molecular junctions; these approaches are also described below.

3.1. In Situ Ultraviolet-Visible Absorption Spectroscopy of Molecular Junctions

Arrangements for in situ spectroscopy of molecular junctions are illustrated in **Figure 2** for transmission (**Figure 2*a*,*b***) and reflectance/scattering (**Figure 2*c*,*d***). In **Figure 2*a***, a semitransparent C film made by pyrolysis (106) or electron-beam deposition (91, 107) is the substrate, and a thin Pt film is the top conductor. The overall transmission of the completed junction is 15–30% for 300–800 nm, and the resulting absorption spectrum obtained with a charge-coupled device–based UV-visible spectrometer is shown in **Figure 8*a***. Because the changes in absorbance during

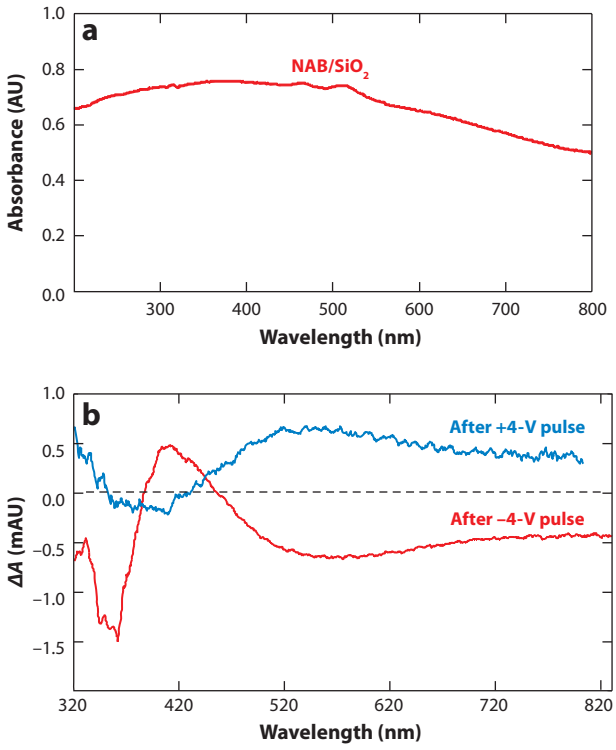

Figure 8

UV-visible spectra of nitroazobenzene (NAB)/SiO_2 molecular junctions obtained in transmission mode. (*a*) Absorbance of junction relative to air, showing minimum transmittance of ~15% at 380 nm. (*b*) Changes in the spectrum of panel *a* in response to ±4-V bias pulses of 100 ms each. Note that the ordinate is in milliabsorbance units (mAU). Reproduced with permission from Reference 91. Copyright American Chemical Society.

junction operation are small, it is useful to plot the absorbance change (ΔA) from the initial curve. **Figure 8*b*** shows plots of ΔA resulting from voltage pulses applied to a C/NAB/SiO_2/Pt molecular junction. The reported detection limit for ΔA was 2×10^{-4}, which corresponds to the expected absorbance of a monolayer ($\sim 5 \times 10^{-10}$ moles cm^{-2}) with a change in molar absorptivity of $\sim$1,000 M^{-1} cm^{-1} (91). These UV-visible results confirmed the reversible reduction of NAB inside the junction and implied that the reduced form is the NAB anion, which had previously been studied by conventional spectroelectrochemistry (55, 90). Simultaneous UV-visible monitoring, accompanying observations of *i-V* behavior, has been applied to polyacetylene in conjugated polymer *p-n* junctions (108, 109) and to conductance changes in polypyrrole-based memory devices. In both cases, the spectroscopic results permitted determination of the doping level of the conducting polymers, including changes that took place during applied bias associated with ion motion (110, 111).

The reflection geometry of **Figure 2*c*** requires only one transparent electrode; it has been employed for both UV-visible and Raman probes of molecular junctions (75, 87). Thin-film interference effects can strongly modulate the responses of both experiments, given that they modify the optical electric field in the vicinity of the absorber or Raman scatterer (112). **Figure 9** shows the transmission spectrum of an $\sim$20-nm-thick film of polythiophene on quartz, showing a maximum absorbance of 0.21 at 557 nm. When the same film is placed on a thick Ag film and a thin

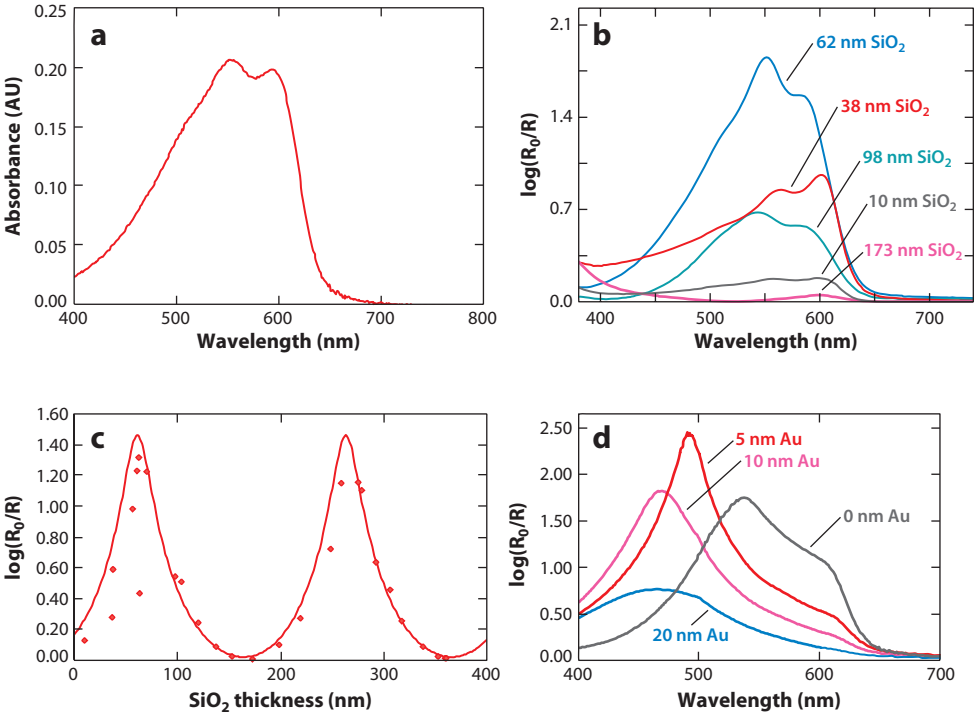

Figure 9

UV-visible spectra for 23-nm-thick polythiophene (PT) films on Ag/SiO_2 surfaces. (*a*) Transmission of PT alone on quartz. (*b*) Reflectance spectra of Ag/SiO_2/PT with varying thicknesses of SiO_2. Note the significantly different absorbance scale from panel *a*. (*c*) Calculated (*line*) and experimental (*points*) reflectance [log(R_o/R)] at 515 nm of Ag/SiO_2/PT devices with a 25-nm-thick PT layer and a 100-nm-thick Ag layer. (*d*) Calculated effect of an Au top contact in complete Ag/SiO_2/PT/Au molecular junctions.

SiO_2 film, the reflectance is strongly modulated by the SiO_2 thickness because of changes in the optical electric field at the polymer layer (**Figure 9*b***). The shape of the spectrum changes within the envelope of the transmission spectrum, and the magnitude of the reflectance is up to 40 times the absorbance determined in transmission geometry. The reflectance can be accurately predicted with standard optical thin-film software (e.g., FilmStar by FTG Software Associates) on the basis of the Fresnel equations and the optical properties of the component films (**Figure 9*c***). The effect of a top contact can also be predicted (**Figure 9*d***). Although such interference effects can complicate the interpretation of reflectance spectra and, to a lesser degree, transmission spectra, they can also be exploited to enhance the spectroscopic response and may lead to optical applications of molecular junctions.

3.2. In Situ Raman Spectroscopy of Molecular Junctions

At first glance, Raman spectroscopy may seem a poor choice for probing molecular junctions, due to its low sensitivity compared with that of UV-visible and FTIR absorption spectroscopy. However, it provides important information about molecular structure, and a wider range of transparent window materials are available for visible versus IR light. Raman spectroelectrochemistry has a long history (90, 104, 113–115); thus, many of the technical issues of interfacing a Raman spectrometer to a thin-layer device have already been addressed in the literature. In addition, surface-enhanced Raman spectroscopy (SERS) can drastically increase the Raman signal, and it is particularly useful for thin-film devices (116–119). Chen et al. (53) obtained SERS spectra in nanowire molecular junctions made with on-wire lithography by exploiting the small wire diameter to generate significant field enhancement (52). The observations were static, but they provided direct evidence for the location and structure of the molecular layer. As mentioned above, SERS has been applied to multilayer films (112) with interference effects in an optimized structure, which provided an additional ~40-fold enhancement over the same SERS structure on a flat glass substrate. Although SERS will probably find significant applications in ME in the future, the tendency of Ag to oxidize and form filaments (120) must be taken into account when Ag nanostructures are used as the enhancing layer. SERS using microfabricated structures or tip-enhanced Raman spectroscopy (121, 122), which circumvents these problems, may prove valuable for monitoring active molecular junctions.

Fortunately, resonance enhancement of Raman scattering results in sufficient sensitivity for probing molecular junctions in situ without the need to rely on metal particles or nanostructures. To date, in situ Raman characterizations have involved the reflection geometry shown in **Figure 2*c***, as well as a charge-coupled device–based spectrometer originally designed to obtain Raman spectra of molecular monolayers on flat electrode surfaces (123). In this study, the resonant Raman-active molecules were NAB and azobenzene (AB), excited at 514.5 nm. Although the instrumentation was conceptually similar to that used for Raman spectroelectrochemistry (90), the sample was very different, consisting of an ~4-nm-thick molecular layer buried in a C/NAB/TiO_2/Au molecular heterojunction with an ~50% transparent, ~15-nm-thick Au top electrode. The scientific question addressed by the experiment was the mechanism of conductance switching, observed for various C/molecule/TiO_2/Au molecular heterojunctions, in which the device switches between high- and low-conductance states by means of a suitable voltage pulse.

Figure 10 shows Raman spectra acquired following the application of bias pulses for a C/NAB/TiO_2/Au molecular junction (87). On the basis of previous spectroelectrochemistry studies in solution (90), an increase in the ratio of intensities for the azo stretches (1,400:1,450 cm^{-1}) has been associated with the reduction of NAB to its anion, which is accompanied by a decrease in the NO_2 stretch intensity at 1,340 cm^{-1}. The resulting spectra permitted several deductions

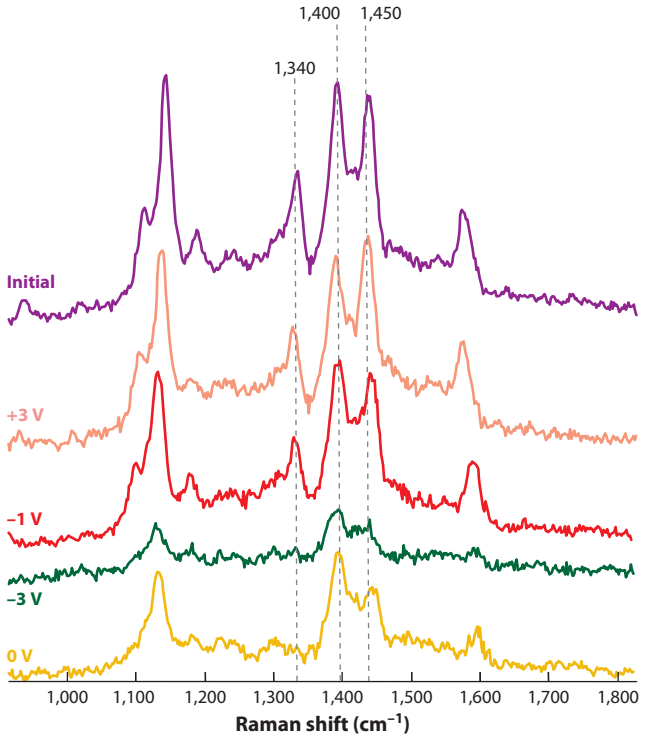

Figure 10

Raman spectra of "live" C/nitroazobenzene/TiO_x/Au molecular junctions obtained with the geometry shown in **Figure 2*c***. Voltage bias values are indicated at the left of each spectrum; they progress chronologically from top to bottom. Reproduced with permission from Reference 87. Copyright American Chemical Society.

about changes in molecular structure caused by the applied bias, which ultimately led to an understanding of the conductance-switching mechanism. First, a negative bias on the C electrode caused electrochemical reduction of the NAB, and the NAB was reoxidized by a positive bias. Second, the reduced NAB was metastable and remained reduced, with zero applied bias, for >60 min. Third, an extreme negative bias caused irreversible loss of the NO_2 stretch, apparently because of the formation of a reduced N center in place of the NO_2 group. Similar spectroscopic effects were observed when TiO_2 was replaced with Al_2O_3, although Al_2O_3 is sufficiently insulating to prevent electronic observation of conductance changes (75, 124). Fourth, the spectroscopic changes in NAB/TiO_2 devices were directly correlated with conductance changes; high conductance occurred with neutral NAB and low conductance with reduced NAB. The combination of the spectroscopic and conductance data led to the conclusion that conductance switching in NAB/TiO_2 is caused by a redox reaction in the TiO_2 that accompanies NAB oxidation and reduction. Because Ti^{III} oxide is $\sim 10^8$ times more conductive than Ti^{IV} oxide, modulation of the Ti oxidation state can cause the large change in observed junction conductance (72, 87, 125, 126).

3.3. Inelastic Tunneling Spectroscopy

IETS was developed in the 1980s to investigate tunnel junctions, which are usually composed of a thin layer of Al_2O_3 on Al and a vapor-deposited top electrode. If a submonolayer of molecules

is deposited between the Al_2O_3 and top electrode, the *i-V* curve for tunneling through the device changes in a subtle but informative way (127–129). Tunneling electrons can interact with the vibrational modes of the molecule, resulting in inelastic tunneling, or orbitals in the molecule can increase the tunneling probability (orbital-mediated tunneling) (130). Such events occur at characteristic voltages that correspond to the energy of the vibrational or electronic transition and appear as small changes in the slope of an otherwise smooth *i-V* curve. The *i-V* curves are usually obtained with a modulated voltage and a lock-in amplifier and are plotted as the second derivative (d^2i/dV^2) to enhance the small changes in slope. The important advantages of IETS include (*a*) the availability of structural information without optical spectroscopy or transparent contacts and (*b*) the fact that IETS is based on the same electron-transport events that underlie the electronic behavior of the junction. Unfortunately, IETS generally requires liquid-He temperatures to avoid broadening of the vibrational features. Thermal broadening at room temperature is ~25 meV, which is sufficient to obscure the small IETS signals [features typically have widths of a few millielectronvolts (131)] unless the sample is cooled to temperatures well below the liquid-N_2 range; the value of the Boltzmann constant (8.617×10^{-5} eV per degree Kelvin) times T at 77 K is 6.6 meV. Given that the range of the vibrational spectrum, 400–4,000 cm^{-1}, corresponds to 0.05–0.5 eV, a typical molecular vibration occurs within a few tenths of an electronvolt of $V = 0$.

IETS provides a great deal of information when used on single-molecule junctions (132, 133) because it is one of very few techniques applicable to single molecules that can provide information about vibrational or electronic transitions. It can be readily achieved via scanning-probe techniques (22, 134) and is an excellent verification of the presence of the molecule, provided that the experiment can be cooled to a low enough temperature to produce observable IETS features. A crossed-wire junction consisting of several thousand molecules suspended between 10-μm-diameter Au wires is also amenable to IETS (135, 136) and has been characterized electronically (94, 137, 138). Wang et al. (139) reported IETS spectra for Si/molecule/Au junctions with areas ranging from 4 to 120 μm^2, including those for a C_{18} alkane layer and a nitrobenzene molecular layer (**Figure 11**). The IETS responses (d^2i/dV^2) ranged from 0.1 to 50 μA, and most of the observed peaks were readily assigned to vibrational modes of the relevant molecules. These

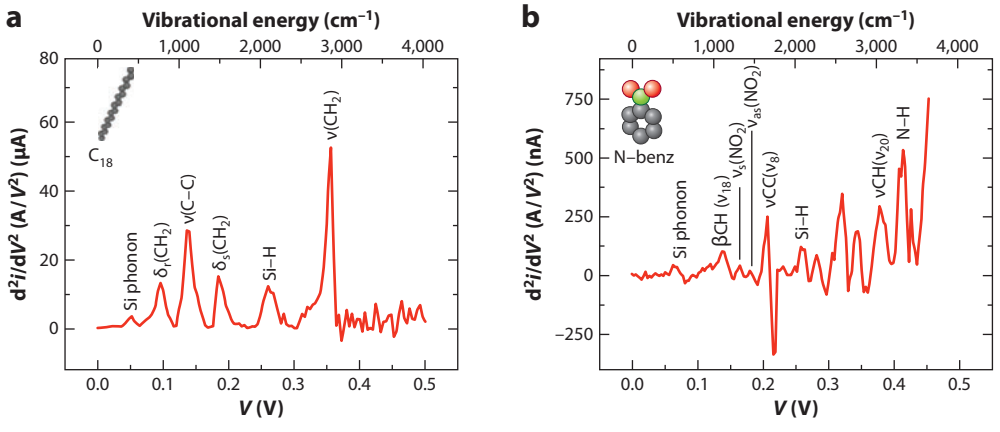

Figure 11

Inelastic tunneling spectroscopy (IETS) spectra of Si/molecule/Au molecular junctions obtained at 4.2 K. The voltage axis is presented as both the bias voltage (*lower axis labels*) and the equivalent vibrational energy (*upper axis labels*). Vibrational assignments of IETS features are indicated on the plots for a molecular layer of (*a*) C_{18} alkane and (*b*) nitrobenzene. Reproduced with permission from Reference 139. Copyright American Chemical Society.

results demonstrate that IETS is applicable to molecular junctions that contain at least thousands of molecules, although the extent of inhomogeneous broadening in so-called ensemble junctions is not known.

4. SUMMARY

The difficulty of characterizing very thin molecular layers or single molecules between conducting contacts in molecular electronic devices has impeded progress in the field due to differences between the actual and intended device structures (12–14). The history of chemistry illustrates the strong synergy between structural characterization and mechanistic understanding, and a similar synergy is likely to continue in ME. As emphasized herein, analytical chemistry plays a major role both during device fabrication and in monitoring working molecular electronic devices. As the field of ME grows, we anticipate continued applications of a range of analytical techniques to ensure that the intended structures are fabricated and the electronic behavior is understood mechanistically. Ultimately, the problem is one of correlating the structure of the molecule in the junction with its behavior—a theme that permeates much of the field of chemistry.

DISCLOSURE STATEMENT

The authors are not aware of any affiliations, memberships, funding, or financial holdings that might be perceived as affecting the objectivity of this review.

ACKNOWLEDGMENTS

Research from the authors' lab was supported by the Natural Sciences and Engineering Research Council, the National Research Council, the National Institute for Nanotechnology (NINT), and the University of Alberta, all in Canada. Research prior to 2006 was supported by the U.S. National Science Foundation and The Ohio State University. The authors appreciate the efforts of Ken Harris, Sudip Barman, Haijun Yan, and Peng Li, who prepared samples for and conducted the scanning electron microscopy, focused ion beam, and transmission electron microscopy analysis in the NINT electron microscopy facility. The authors also thank Lian C.T. Shoute for acquiring some of the data shown in **Figure 9**.

LITERATURE CITED

1. Akkerman HB, Blom PWM, de Leeuw DM, de Boer B. 2006. Towards molecular electronics with large-area molecular junctions. *Nature* 441:69–72
2. Akkerman HB, De Boer B. 2008. Electrical conduction through single molecules and self-assembled monolayers. *J. Phys. Condens. Matter* 20:013001
3. Chen F, Hihath J, Huang Z, Li X, Tao NJ. 2007. Measurement of single molecule conductance. *Annu. Rev. Phys. Chem.* 58:535–64
4. Green JE, Wook Choi J, Boukai A, Bunimovich Y, Johnston-Halperin E, et al. 2007. A 160-kilobit molecular electronic memory patterned at 1,011 bits per square centimetre. *Nature* 445:414–17
5. Haick H, Cahen D. 2008. Contacting organic molecules by soft methods: towards molecule-based electronic devices. *Acc. Chem. Res.* 41:359–66
6. Kronemeijer AJ, Akkerman HB, Kudernac T, van Wees BJ, Feringa BL, et al. 2008. Reversible conductance switching in molecular devices. *Adv. Mater.* 20:1467–73
7. Liu Y, Flood A, Stoddart JF. 2004. Thermally and electrochemically controllable self-complexing molecular switches. *J. Am. Chem. Soc.* 126:9150–51

8. McCreery R. 2004. Molecular electronic junctions. *Chem. Mater.* 16:4477–96
9. Selzer Y, Allara D. 2006. Single-molecule electrical junctions. *Annu. Rev. Phys. Chem.* 57:593–623
10. Vilan A, Yaffe O, Biller A, Salomon A, Kahn A, Cahen D. 2010. Molecules on Si: electronics with chemistry. *Adv. Mater.* 22:140–59
11. Yaffe O, Scheres L, Puniredd SR, Stein N, Biller A, et al. 2009. Molecular electronics at metal/semiconductor junctions. Si inversion by sub-nanometer molecular films. *Nano Lett.* 9:2390–94
12. McCreery RL. 2006. Analytical challenges in molecular electronics. *Anal. Chem.* 78:3490–97
13. McCreery RL, Bergren AJ. 2009. Progress with molecular electronic junctions: meeting experimental challenges in design and fabrication. *Adv. Mater.* 21:4303–22
14. Batteas JD, Chidsey CED, Kagan CR, Seideman T. 2007. *Building electronic function into nanoscale molecular architectures*. Presented at Natl. Sci. Found. Workshop, Ballston, Va. **http://wtec.org/MolecularElectronics/MolecularElectronics-enc.pdf**
15. Dickie AJ, Wolkow RA. 2008. Metal-organic-silicon nanoscale contacts. *Phys. Rev. B* 77:115305–6
16. Kim WY, Choi YC, Min SK, Cho Y, Kim KS. 2009. Application of quantum chemistry to nanotechnology: electron and spin transport in molecular devices. *Chem. Soc. Rev.* 38:2319–33
17. Piva PG, DiLabio GA, Pitters JL, Zikovsky J, Rezeq MD, et al. 2005. Field regulation of single-molecule conductivity by a charged surface atom. *Nature* 435:658–61
18. Qiu XH, Nazin GV, Ho W. 2003. Vibrationally resolved fluorescence excited with submolecular precision. *Science* 299:542–46
19. Sinha S, Dickie AJ, Wolkow RA. 2009. Tuning tunneling current rectification with chemical modification of silicon(100) surfaces. *Chem. Phys. Lett.* 469:279–83
20. Tu XW, Mikaelian G, Ho W. 2008. Controlling single-molecule negative differential resistance in a double-barrier tunnel junction. *Phys. Rev. Lett.* 100:126807
21. Zaumseil J, Ho X, Guest JR, Wiederrecht GP, Rogers JA. 2009. Electroluminescence from electrolyte-gated carbon nanotube field-effect transistors. *Am. Chem. Soc. Nano* 3:2225–34
22. Moore A, Weiss PS. 2008. Functional and spectroscopic measurements with scanning tunneling microscopy. *Annu. Rev. Anal. Chem.* 1:857–82
23. Schmid SA, Yim KH, Chang MH, Zheng Z, Huck WTS, et al. 2008. Polarization anisotropy dynamics for thin films of a conjugated polymer aligned by nanoimprinting. *Phys. Rev. B* 77:115338
24. Kaake LG, Zou Y, Panzer MJ, Frisbie CD, Zhu XY. 2007. Vibrational spectroscopy reveals electrostatic and electrochemical doping in organic thin film transistors gated with a polymer electrolyte dielectric. *J. Am. Chem. Soc.* 129:7824–30
25. Lindsay SM, Ratner MA. 2007. Molecular transport junctions: clearing mists. *Adv. Mater.* 19:23–31
26. Metzger RM. 2006. Unimolecular rectifiers: present status. *Chem. Phys.* 326:176–87
27. Salomon A, Cahen D, Lindsay S, Tomfohr J, Engelkes VB, Frisbie CD. 2003. Comparison of electronic transport measurements on organic molecules. *Adv. Mater.* 15:1881–90
28. Chen F, Tao NJ. 2009. Electron transport in single molecules: from benzene to graphene. *Acc. Chem. Res.* 42:429–38
29. Del Nero J, de Souza FM, Capaz RB. 2010. Molecular electronics devices: a short review. *J. Comput. Theor. Nanosci.* 7:503–16
30. Erbe A, Verleger S. 2009. Molecular electronics: a review of experimental results. *Acta Phys. Polon. A* 115:455–61
31. Grigoriev A, Ahuja R. 2007. Molecular electronics devices. See Ref. 34, pp. 25.1–25.34
32. Heath JR. 2009. Molecular electronics. *Annu. Rev. Mater. Res.* 39:1–23
33. Hussain SA, Bhattacharjee D. 2009. Langmuir-Blodgett films and molecular electronics. *Mod. Phys. Lett. B* 23:3437–51
34. Lyshevski SE, ed. 2007. *Nano and Molecular Electronics Handbook*. Boca Raton: CRC
35. Metzger RM. 2003. Unimolecular electrical rectifiers. *Chem. Rev.* 103:3803–34
36. Moth-Poulsen K, Bjornholm T. 2009. Molecular electronics with single molecules in solid-state devices. *Nat. Nanotechnol.* 4:551–56
37. James DK, Tour JM. 2004. Electrical measurements in molecular electronics. *Chem. Mater.* 16:4423–35
38. Anariba F, McCreery RL. 2002. Electronic conductance behavior of carbon-based molecular junctions with conjugated structures. *J. Phys. Chem. B* 106:10355–62

39. Anariba F, Steach J, McCreery R. 2005. Strong effects of molecular structure on electron transport in carbon/molecule/copper electronic junctions. *J. Phys. Chem. B* 109:11163–72
40. Bergren AJ, Harris KD, Deng F, McCreery R. 2008. Molecular electronics using diazonium-derived adlayers on carbon with Cu top contacts: critical analysis of metal oxides and filaments. *J. Phys. Condens. Matter* 20:374117
41. Bergren AJ, McCreery RL, Stoyanov SR, Gusarov S, Kovalenko A. 2010. Electronic characteristics and charge transport mechanisms for large area aromatic molecular junctions. *J. Phys. Chem. C* 114:15806–15
42. Chiechi RC, Weiss EA, Dickey MD, Whitesides GM. 2008. Eutectic gallium-indium (EGaIn): a moldable liquid metal for electrical characterization of self-assembled monolayers. *Angew. Chem. Int. Ed.* 47:142–44
43. Coll M, Miller LH, Richter LJ, Hines DR, Jurchescu OD, et al. 2009. Formation of silicon-based molecular electronic structures using flip-chip lamination. *J. Am. Chem. Soc.* 131:12451–57
44. DeIonno E, Tseng HR, Harvey DD, Stoddart JF, Heath JR. 2006. Infrared spectroscopic characterization of [2]rotaxane molecular switch tunnel junction devices. *J. Phys. Chem. B* 110:7609–12
45. Nijhuis CA, Reus WF, Barber JR, Dickey MD, Whitesides GM. 2010. Charge transport and rectification in arrays of SAM-based tunneling junctions. *Nano Lett.* 10:3611–19
46. Nijhuis CA, Reus WF, Whitesides GM. 2009. Molecular rectification in metal SAM–metal oxide–metal junctions. *J. Am. Chem. Soc.* 131:17814–27
47. Ranganathan S, Steidel I, Anariba F, McCreery RL. 2001. Covalently bonded organic monolayers on a carbon substrate: a new paradigm for molecular electronics. *Nano Lett.* 1:491–94
48. Richter CA, Hacker CA, Richter LJ. 2005. Electrical and spectroscopic characterization of metal/monolayer/Si devices. *J. Phys. Chem. B* 109:21836
49. Richter CA, Hacker CA, Richter LJ, Vogel EM. 2004. Molecular devices formed by direct monolayer attachment to silicon. *Solid State Electron.* 48:1747–52
50. Scott A, Hacker CA, Janes DB. 2008. In situ structural characterization of metal/molecule/silicon junctions using backside infrared spectroscopy. *J. Phys. Chem. C* 112:14021–26
51. Wong EW, Collier CP, Behloradsky M, Raymo FM, Stoddart JF, Heath JR. 2000. Fabrication and transport properties of single-molecule-thick electrochemical junctions. *J. Am. Chem. Soc.* 122:5831–40
52. Chen X, Braunschweig AB, Wiester MJ, Yeganeh S, Ratner MA, Mirkin CA. 2009. Spectroscopic tracking of molecular transport junctions generated by using click chemistry. *Angew. Chem. Int. Ed.* 48:5178–81
53. Chen X, Jeon Y-M, Jang J-W, Qin L, Huo F, et al. 2008. On-wire lithography-generated molecule-based transport junctions: a new testbed for molecular electronics. *J. Am. Chem. Soc.* 130:8166–68
54. Pandey D, Zemlyanov DY, Bevan K, Reifenberger RG, Dirk SM, et al. 2007. UHV STM I(V) and XPS studies of aryl diazonium molecules assembled on Si(111). *Langmuir* 23:4700–8
55. Tian H, Bergren AJ, McCreery RL. 2007. Ultraviolet visible spectroelectrochemistry of chemisorbed molecular layers on optically transparent carbon electrodes. *Appl. Spectrosc.* 61:1246–53
56. Anariba F, DuVall SH, McCreery RL. 2003. Mono- and multilayer formation by diazonium reduction on carbon surfaces monitored with atomic force microscopy "scratching". *Anal. Chem.* 75:3837–44
57. Edwards GA, Bergren AJ, Porter MD. 2007. Chemically modified electrodes. In *Handbook of Electrochemistry*, ed. CG Zoski, pp. 295–327. New York: Elsevier
58. Murray RW. 1980. Chemically modified electrodes. *Acc. Chem. Res.* 13:135–41
59. Murray RW. 1983. Chemically modified electrodes. In *Electroanalytical Chemistry*, ed. A Bard, pp. 191–368. New York: Marcel Dekker
60. Scott A, Janes DB, Risko C, Ratner MA. 2007. Fabrication and characterization of metal-molecule-silicon devices. *Appl. Phys. Lett.* 91:033508
61. Seo K, Lee H. 2009. Molecular electron transport changes upon structural phase transitions in alkanethiol molecular junctions. *Am. Chem. Soc. Nano* 3:2469–76
62. Kariuki JK, McDermott MT. 1999. Nucleation and growth of functionalized aryl films on graphite electrodes. *Langmuir* 15:6534–40
63. Kariuki JK, McDermott MT. 2001. Formation of multilayers on glassy carbon electrodes via the reduction of diazonium salts. *Langmuir* 17:5947–51

64. Liscio A, Palermo V, Samori P. 2010. Nanoscale quantitative measurement of the potential of charged nanostructures by electrostatic and Kelvin probe force microscopy: unraveling electronic processes in complex materials. *Acc. Chem. Res.* 43:541–50
65. Yan H, McCreery RL. 2009. Anomalous tunneling in carbon/alkane/TiO_2/gold molecular electronic junctions: energy level alignment at the metal/semiconductor interface. *Am. Chem. Soc. Appl. Mater. Interfaces* 1:443–51
66. Takano H, Porter MD. 2001. Monitoring chemical transformations at buried organic interfaces by electric force microscopy. *J. Am. Chem. Soc.* 123:8412–13
67. Takano H, Wong S-S, Harnisch JA, Porter MD. 2000. Mapping the subsurface composition of organic film by electric force microscopy. *Langmuir* 16:5231–33
68. Melitz W, Shen J, Lee S, Lee JS, Kummel AC, et al. 2010. Scanning tunneling spectroscopy and Kelvin probe force microscopy investigation of Fermi energy level pinning mechanism on InAs and InGaAs clean surfaces. *J. Appl. Phys.* 108:023711
69. Marshall GM, Lopinski GP, Bensebaa F, Dubowski JJ. 2009. Surface dipole layer potential induced IR absorption enhancement in n-alkanethiol SAMs on GaAs(001). *Langmuir* 25:13561–68
70. Seitz O, Dai M, Aguirre-Tostado FS, Wallace RM, Chabal YJ. 2009. Copper-metal deposition on self assembled monolayer for making top contacts in molecular electronic devices. *J. Am. Chem. Soc.* 131:18159–67
71. Seitz O, Vilan A, Cohen H, Hwang J, Haeming M, et al. 2008. Doping molecular monolayers: effects on electrical transport through alkyl chains on silicon. *Adv. Funct. Mater.* 18:2102–13
72. McCreery R, Wu J, Kalakodimi RJ. 2006. Electron transport and redox reactions in carbon based molecular electronic junctions. *Phys. Chem. Chem. Phys.* 8:2572–90
73. McGovern WR, Anariba F, McCreery R. 2005. Importance of oxides in carbon/molecule/metal molecular junctions with titanium and copper top contacts. *J. Electrochem. Soc.* 152:E176–83
74. Nowak AM, McCreery RL. 2004. Characterization of carbon/nitroazobenzene/titanium molecular electronic junctions with photoelectron and Raman spectroscopy. *Anal. Chem.* 76:1089–97
75. Kalakodimi RP, Nowak A, McCreery RL. 2005. Carbon/molecule/metal and carbon/molecule/metal oxide molecular electronic junctions. *Chem. Mater.* 17:4939–48
76. Walker AV, Tighe TB, Cabarcos OM, Reinard MD, Haynie BC, et al. 2004. The dynamics of noble metal atom penetration through methoxy-terminated alkanethiolate monolayers. *J. Am. Chem. Soc.* 126:3954–63
77. Walker AV, Tighe TB, Haynie BC, Uppili S, Winograd N, Allara D. 2005. Chemical pathways in the interactions of reactive metal atoms with organic surfaces: vapor deposition of Ca and Ti on a methoxy-terminated alkanethiolate monolayer on Au. *J. Phys. Chem. B* 109:11263–72
78. Zhu Z, Daniel TA, Maitani M, Cabarcos OM, Allara DL, Winograd N. 2006. Controlling gold atom penetration through alkanethiolate self-assembled monolayers on Au{111} by adjusting terminal group intermolecular interactions. *J. Am. Chem. Soc.* 128:13710–19
79. Kim B, Beebe JM, Jun Y, Zhu XY, Frisbie CD. 2006. Correlation between HOMO alignment and contact resistance in molecular junctions: aromatic thiols versus aromatic isocyanides. *J. Am. Chem. Soc.* 128:4970–71
80. Schalnat MC, Pemberton JE. 2010. Comparison of a fluorinated aryl thiol self-assembled monolayer with its hydrogenated counterpart on polycrystalline Ag substrates. *Langmuir* 26:11862–69
81. Seitz O, Vilan A, Cohen H, Chan C, Hwang J, et al. 2007. Effect of doping on electronic transport through molecular monolayer junctions. *J. Am. Chem. Soc.* 129:7494–95
82. Huisman EH, Guedon CM, van Wees BJ, Van Der Molen SJ. 2009. Interpretation of transition voltage spectroscopy. *Nano Lett.* 9:3909–13
83. Donley CL, Blackstock JJ, Stickle WF, Stewart DR, Williams RS. 2007. In-situ infrared spectroscopy of buried organic monolayers: influence of the substrate on titanium reactivity with a Langmuir-Blodgett film. *Langmuir* 23:7620–25
84. Mahmoud AM, Bergren AJ, McCreery RL. 2009. Derivatization of optically transparent materials with diazonium reagents for spectroscopy of buried interfaces. *Anal. Chem.* 81:6972–80

85. Allongue P, Henry de Villeneuve C, Cherouvrier G, Cortes R, Bernard MC. 2003. Phenyl layers on H-Si(111) by electrochemical reduction of diazonium salts: monolayer versus multilayer formation. *J. Electroanal. Chem.* 550–551:161–74
86. Henry de Villeneuve C, Pinson J, Bernard MC, Allongue P. 1997. Electrochemical formation of close-packed phenyl layers on Si(111). *J. Phys. Chem. B* 101:2415–20
87. Nowak A, McCreery R. 2004. In-situ Raman spectroscopy of bias-induced structural changes in nitroazobenzene molecular electronic junctions. *J. Am. Chem. Soc.* 126:16621–31
88. Tian JH, Liu B, Li XL, Yang ZL, Ren B, et al. 2006. Study of molecular junctions with a combined surface-enhanced Raman and mechanically controllable break junction method. *J. Am. Chem. Soc.* 128:14748–49
89. Yoon HP, Maitani MM, Cabarcos OM, Cai L, Mayer TS, Allara DL. 2010. Crossed-nanowire molecular junctions: a new multispectroscopy platform for conduction-structure correlations. *Nano Lett.* 10:2897–902
90. Itoh T, McCreery RL. 2002. In situ Raman spectroelectrochemistry of electron transfer between glassy carbon and a chemisorbed nitroazobenzene monolayer. *J. Am. Chem. Soc.* 124:10894–902
91. Bonifas AP, McCreery RL. 2008. In-situ optical absorbance spectroscopy of molecular layers in carbon based molecular electronic devices. *Chem. Mater.* 20:3849–56
92. Douvas AM, Makarona E, Glezos N, Argitis P, Mielczarski JA, Mielczarski E. 2008. Polyoxometalate-based layered structures for charge transport control in molecular devices. *Am. Chem. Soc. Nano* 2:733–42
93. Liang H, Tian H, McCreery RL. 2007. Normal and surface-enhanced Raman spectroscopy of nitroazobenzene submonolayers and multilayers on carbon and silver surfaces. *Appl. Spectrosc.* 61:613
94. Beebe JM, Kim B, Frisbie CD, Kushmerick JG. 2008. Measuring relative barrier heights in molecular electronic junctions with transition voltage spectroscopy. *Am. Chem. Soc. Nano* 2:827–32
95. Choi SH, Kim B, Frisbie CD. 2008. Electrical resistance of long conjugated molecular wires. *Science* 320:1482–86
96. Choi SH, Risko C, Delgado MCR, Kim B, Bredas J-L, Frisbie CD. 2010. Transition from tunneling to hopping transport in long, conjugated oligo-imine wires connected to metals. *J. Am. Chem. Soc.* 132:4358–68
97. Maitani MM, Allara DL, Ohlberg DAA, Li Z, Williams RS, Stewart DR. 2010. High integrity metal/organic device interfaces via low temperature buffer layer assisted metal atom nucleation. *Appl. Phys. Lett.* 96:173109
98. Maitani MM, Daniel TA, Cabarcos OM, Allara DL. 2009. Nascent metal atom condensation in self-assembled monolayer matrices: coverage-driven morphology transitions from buried adlayers to electrically active metal atom nanofilaments to overlayer clusters during aluminum atom deposition on alkanethiolate/gold monolayers. *J. Am. Chem. Soc.* 131:8016–29
99. Bonifas AP, McCreery RL. 2010. "Soft" Au, Pt and Cu contacts for molecular junctions through surface-diffusion-mediated deposition. *Nat. Nanotechnol.* 5:612–17
100. Strachan JP, Matthew DP, Yang JJ, Shaul A, Kilcoyne ALD, et al. 2010. Direct identification of the conducting channels in a functioning memristive device. *Adv. Mater.* 22:3573–77
101. Kuikka MA, Li W, Kavanagh KL, Yu H-Z. 2008. Nanoscale electrical and structural characterization of gold/alkyl monolayer/silicon diode junctions. *J. Phys. Chem. C* 112:9081–88
102. Solak AO, Eichorst LR, Clark WJ, McCreery RL. 2003. Modified carbon surfaces as "organic electrodes" that exhibit conductance switching. *Anal. Chem.* 75:296–305
103. McCreery RL, Dieringer J, Solak AO, Snyder B, Nowak A, et al. 2003. Molecular rectification and conductance switching in carbon based molecular junctions by structural rearrangement accompanying electron injection. *J. Am. Chem. Soc.* 125:10748–58
104. Gale RJ. 1988. *Spectroelectrochemistry: Theory and Practice*. New York: Plenum
105. McCreery RL. 1986. Spectroelectrochemistry. In *Physical Methods in Chemistry*, ed. B Rossiter, pp. 591–662. New York: Wiley
106. Donner S, Li HW, Yeung ES, Porter MD. 2006. Fabrication of optically transparent carbon electrodes by the pyrolysis of photoresist films: approach to single-molecule spectroelectrochemistry. *Anal. Chem.* 78:2816–22
107. Blackstock JJ, Rostami AA, Nowak AM, McCreery RL, Freeman M, McDermott MT. 2004. Ultraflat carbon film electrodes prepared by electron beam evaporation. *Anal. Chem.* 76:2544–52

108. Cheng CH, Lin F, Lonergan MC. 2005. Charge transport in a mixed ionically/electronically conducting, cationic, polyacetylene ionomer between ion-blocking electrodes. *J. Phys. Chem. B.* 109:10168–78
109. Cheng CHW, Lonergan MC. 2004. A conjugated polymer pn junction. *J. Am. Chem. Soc.* 126:10536–37
110. Rahman GMA, Zhao J-H, Thomson DJ, Freund MS. 2009. Compensation doping in conjugated polymers: engineering dopable heterojunctions for modulating conductivity in the solid state. *J. Am. Chem. Soc.* 131:15600–1
111. Zhao JH, Thomson DJ, Pilapil M, Pillai RG, Rahman GMA, Freund MS. 2010. Field enhanced charge carrier reconfiguration in electronic and ionic coupled dynamic polymer resistive memory. *Nanotechnology* 21:134003
112. Shoute LCT, Bergren AJ, Mahmoud AM, Harris KD, McCreery RL. 2009. Optical interference effects in the design of substrates for surface-enhanced Raman spectroscopy. *Appl. Spectrosc.* 63:133–40
113. Allen CS, Schatz GC, Van Duyne RP. 1980. Tunable laser excitation profile of surface enhanced Raman scattering from pyridine adsorbed on a copper electrode surface. *Chem. Phys. Lett.* 75:201–5
114. Packard RT, McCreery RL. 1988. Raman monitoring of reactive electrogenerated species: kinetics of halide addition to orthoquinones. *J. Phys. Chem.* 92:6345–51
115. Van Duyne RP, Haushalter JP. 1984. Resonance Raman spectroelectrochemistry of semiconductor electrodes: the photooxidation of tetrathiafulvalene at n-GaAs(100) in acetonitrile. *J. Phys. Chem.* 88:2446–51
116. Dieringer JA, Wustholz KL, Masiello DJ, Camden JP, Kleinman SL, et al. 2009. Surface-enhanced Raman excitation spectroscopy of a single rhodamine 6G molecule. *J. Am. Chem. Soc.* 131:849–54
117. Haes AJ, Zou S, Schatz GC, Van Duyne RP. 2004. Nanoscale optical biosensor: short range distance dependence of the localized surface plasmon resonance of noble metal nanoparticles. *J. Phys. Chem. B* 108:6161–68
118. Lacy WB, Olson LG, Harris JM. 1999. Quantitative SERS measurements on dielectric-overcoated silver-island films by solution-deposition control of surface concentrations. *Anal. Chem.* 71:2564–70
119. Zhao J, Dieringer JA, Zhang X, Schatz GC, Van Duyne RP. 2008. Wavelength-scanned surface-enhanced resonance Raman excitation spectroscopy. *J. Phys. Chem. C* 112:19302–10
120. Ssenyange S, Yan H, McCreery RL. 2006. Redox-driven conductance switching via filament formation and dissolution in carbon/molecule/TiO_2/Ag molecular electronic junctions. *Langmuir* 22:10689–96
121. Olk P, Renger J, Hartling T, Wenzel MT, Eng LM. 2007. Two particle enhanced nano Raman microscopy and spectroscopy. *Nano Lett.* 7:1736–40
122. Zhang W, Yeo BS, Schmid T, Zenobi R. 2007. Single molecule tip-enhanced Raman spectroscopy with silver tips. *J. Phys. Chem. C* 111:1733–38
123. Ramsey JD, Ranganathan S, Zhao J, McCreery RL. 2001. Performance comparison of conventional and line-focused surface Raman spectrometers. *Appl. Spectrosc.* 55:767–73
124. McCreery RL, Viswanathan U, Kalakodimi RP, Nowak AM. 2006. Carbon/molecule/metal molecular electronic junctions: the importance of "contacts". *Faraday Discuss.* 131:33–43
125. Wu J, McCreery RL. 2009. Solid-state electrochemistry in molecule/TiO_2 molecular heterojunctions as the basis of the TiO_2 "Memristor". *J. Electrochem. Soc.* 156:P29–37
126. Wu J, Mobley K, McCreery R. 2007. Electronic characteristics of fluorene/TiO_2 molecular heterojunctions. *J. Chem. Phys.* 126:24704
127. Hipps KW, Mazur U. 2002. Inelastic electron tunneling spectroscopy. In *Handbook of Vibrational Spectroscopy*, ed. JM Chalmers, PR Griffiths, pp. 812–29. Chichester, UK: Wiley
128. Hoagland JJ, Wang XD, Hipps KW. 1993. Characterization of Cu-CuTCNQ-M devices using scanning electron microscopy and scanning tunneling microscopy. *Chem. Mater.* 5:54–60
129. Scudiero L, Barlow DE, Mazur U, Hipps KW. 2001. Scanning tunneling microscopy, orbital-mediated tunneling spectroscopy, and ultraviolet photoelectron spectroscopy of metal(II) tetraphenylporphyrins deposited from vapor. *J. Am. Chem. Soc.* 123:4073–80
130. Mazur U, Hipps KW. 1999. Orbital-mediated tunneling, inelastic electron tunneling, and electrochemical potentials for metal phthalocyanine thin films. *J. Phys. Chem. B* 103:9721–27
131. Galperin M, Ratner MA, Nitzan A. 2004. On the line widths of vibrational features in inelastic electron tunneling spectroscopy. *Nano Lett.* 4:1605–11

132. Leng J-C, Lin LL, Song X-N, Li Z-L, Wang C-K. 2009. Orientation of decanethiol molecules in self-assembled monolayers determined by inelastic electron tunneling spectroscopy. *J. Phys. Chem. C* 113:18353–57
133. Selzer Y, Cabassi MA, Mayer TS, Allara DL. 2004. Thermally activated conduction in molecular junctions. *J. Am. Chem. Soc.* 126:4052–53
134. Hofer WA, Fisher AJ, Lopinski GP, Wolkow RA. 2002. Electronic structure and STM images of self-assembled styrene lines on a Si(100) surface. *Chem. Phys. Lett.* 365:129–34
135. Troisi A, Beebe JM, Picraux LB, van Zee RD, Stewart DR, et al. 2007. Tracing electronic pathways in molecules by using inelastic tunneling spectroscopy. *Proc. Natl. Acad. Sci. USA* 104:14255–59
136. Troisi A, Ratner MA. 2006. Molecular transport junctions: propensity rules for inelastic electron tunneling spectra. *Nano Lett.* 6:1784–88
137. Beebe JM, Kim B, Gadzuk JW, Frisbie CD, Kushmerick JG. 2006. Transition from direct tunneling to field emission in metal-molecule-metal junctions. *Phys. Rev. Lett.* 97:026801
138. Kim BS, Beebe JM, Olivier C, Rigaut S, Touchard D, et al. 2007. Temperature and length dependence of charge transport in redox-active molecular wires incorporating ruthenium(II) bis(σ-arylacetylide) complexes. *J. Phys. Chem. C* 111:7521–26
139. Wang W, Scott A, Gergel-Hackett N, Hacker CA, Janes DB, Richter CA. 2008. Probing molecules in integrated silicon-molecule-metal junctions by inelastic tunneling spectroscopy. *Nano Lett.* 8:478–84
140. Ru J, Szeto B, Bonifas A, McCreery RL. 2010. Microfabrication and integration of diazonium-based aromatic molecular junctions. *Am. Chem. Soc. Appl. Mater. Interfaces* 2:3693–701
141. Barman S, Deng F, McCreery R. 2008. Conducting polymer memory devices based on dynamic doping. *J. Am. Chem. Soc.* 130:11073–81

Annual Review of
Analytical Chemistry

Volume 4, 2011

Contents

Indexes

Errata

An online log of corrections to the *Annual Review of Analytical Chemistry* articles may be found at http://arjournals.annualreviews.org/errata/anchem